Virologica Sinica 38 (2023) 508–519

Contents lists available at ScienceDirect

Virologica Sinica

journal homepage: www.keaipublishing.com/en/journals/virologica-sinica
www.virosin.org

Research Article

Integrated interactome and transcriptome analysis reveals key host factors critical for SARS-CoV-2 infection

Jie Sheng [a,b,c,1], Lili Li [a,b,1], Xueying Lv [a,b,d], Meiling Gao [a,b], Ziyi Chen [a,b], Zhuo Zhou [a,b], Jingfeng Wang [a,b,*], Aiping Wu [a,b,*], Taijiao Jiang [a,b,e,f,*]

[a] Institute of Systems Medicine, Chinese Academy of Medical Sciences & Peking Union Medical College, Beijing, 100005, China
[b] Suzhou Institute of Systems Medicine, Suzhou, 215123, China
[c] Institute of Basic Medical Sciences, Chinese Academy of Medical Sciences, School of Basic Medicine, Peking Union Medical College, Beijing, 100005, China
[d] Department of Microbiology and Parasitology, College of Basic Medical Sciences, China Medical University, Shenyang, 110122, China
[e] Guangzhou Laboratory, Guangzhou, 510005, China
[f] State Key Laboratory of Respiratory Disease, the First Affiliated Hospital of Guangzhou Medical University, Guangzhou Medical University, Guangzhou, 510120, China

ARTICLE INFO

Keywords:
SARS-CoV-2
Interactome
Transcriptome
Integration analysis
ER stress

ABSTRACT

The coronavirus disease 2019 (COVID-19) pandemic, caused by severe acute respiratory syndrome coronavirus 2 (SARS-CoV-2), has seriously threatened global public health and caused huge economic losses. Omics studies of SARS-CoV-2 can help understand the interaction between the virus and host, thereby providing a new perspective in guiding the intervention and treatment of the SARS-CoV-2 infection. Since large amount of SARS-CoV-2 omics data have been accumulated in public databases, this study aimed to identify key host factors involved in SARS-CoV-2 infection through systematic integration of transcriptome and interactome data. By manually curating published studies, we obtained a comprehensive SARS-CoV-2-human protein-protein interactions (PPIs) network, comprising 3591 human proteins interacting with 31 SARS-CoV-2 viral proteins. Using the RobustRankAggregation method, we identified 123 multiple cell line common genes (CLCGs), of which 115 up-regulated CLCGs showed host enhanced innate immunity and chemotactic response signatures. Combined with network analysis, co-expression and functional enrichment analysis, we discovered four key host factors involved in SARS-CoV-2 infection: IFITM1, SERPINE1, DDX60, and TNFAIP2. Furthermore, SERPINE1 was found to facilitate SARS-CoV-2 replication, and can alleviate the endoplasmic reticulum (ER) stress induced by ORF8 protein through interaction with ORF8. Our findings highlight the importance of systematic integration analysis in understanding SARS-CoV-2-human interactions and provide valuable insights for future research on potential therapeutic targets against SARS-CoV-2 infection.

1. Introduction

In the past two decades, coronaviruses have caused three large-scale outbreaks: severe acute respiratory syndrome (SARS), Middle East respiratory syndrome (MERS) and recently severe acute respiratory syndrome coronavirus 2 (SARS-CoV-2) (Harrison et al., 2020). In December 2019, the first coronavirus disease 2019 (COVID-19) case was reported (Huang et al., 2020), and rapid human-to-human and intercontinental transmission were subsequently discovered. It was declared as a pandemic by the World Health Organization on March 11, 2020 (Cucinotta and Vanelli, 2020). The SARS-CoV-2 outbreak, especially the recent global dissemination of the Omicron variant, has posed a serious threat to global public health, resulting in massive economic losses throughout the world (Araf et al., 2022).

SARS-CoV-2 is a positive-sense single-stranded RNA virus that encodes four structural proteins, sixteen nonstructural proteins (NSPs), and several accessory proteins (Chen et al., 2020; Wu et al., 2020). The structural proteins primarily function in forming infectious virions (Yang and Rao, 2021). NSPs are critical for replication, and accessory proteins are involved in dysregulating host immune responses and modulating host cell signaling pathways (Suryawanshi et al., 2021). The competition between host antiviral immunity and viral antagonism forms the

* Corresponding authors.
E-mail addresses: wangjf@ism.cams.cn (J. Wang), wap@ism.cams.cn (A. Wu), jiang_taijiao@gzlab.ac.cn (T. Jiang).
[1] Jie Sheng and Lili Li contributed equally to this work.

https://doi.org/10.1016/j.virs.2023.05.004
Received 16 January 2023; Accepted 5 May 2023
Available online 9 May 2023

virus-host interaction networks. Although the host activates innate and adaptive immune responses to resist viral infection, viruses develop a variety of strategies to modulate host signaling pathways and hijack host metabolism resources to facilitate their replication (Chen et al., 2022). Investigating the interaction between viral and host proteins is of great significance in understanding the pathogenesis of emerging viruses (Tan et al., 2007). Several individual studies have used large-scale methods to decipher the interplay between SARS-CoV-2 and its hosts. Using affinity-purification mass spectrometry (AP-MS), David E Gordon et al. identified 332 high-confidence SARS-CoV-2 and human protein-protein interactions (PPIs) (Gordon et al., 2020a). Meanwhile, scientists compared virus-human PPIs for SARS-CoV-2, SARS, and MERS, obtained conserved PPIs across all three viruses and identified 73 host factors required for SARS-CoV-2 replication (Gordon et al., 2020b). However, a single PPI study identified only the tip of the iceberg of SARS-CoV-2 interactome. A comprehensive analysis of virus-host interactions is urgently needed. With the emergence of this new virus, a great number of SARS-CoV-2 transcriptome data has been accumulated in public databases (Blanco-Melo et al., 2020b; Ren et al., 2021). Previous studies seemed to be limited and focused mostly on single cell line or tissue. Nevertheless, results from traditional single sequencing data studies suffer from low reproducibility due to the heterogeneity of experimental samples, different sequencing techniques and data processing methods (Aevermann et al., 2014). The integration of various datasets will allow us to acquire a comprehensive perspective of virus-host interactions and expand our understanding on how viral proteins hijack host systems to favor their replication and immune evasion, as well as to identify crucial host factors.

In this study, we conducted a systematic integrated analysis of interactome and transcriptome datasets from different studies, to provide a panoramic view of the interactions between SARS-CoV-2 proteins and human proteins. By combing network analysis, gene ranking, co-expression networks and functional enrichment analysis, we identified four key host factors involved in SARS-CoV-2 infection, including SERPINE1, TNFAIP2, IFITM1 and DDX60. Furthermore, we showed that SERPINE1 can facilitate SARS-CoV-2 replication and can interact with the SARS-CoV-2 ORF8 protein to alleviate the endoplasmic reticulum (ER) stress induced by ORF8. Overall, our findings improve our understanding of SARS-CoV-2 viral protein function and host immunity, paving the way for the development of potential therapeutic strategies.

2. Materials and methods

2.1. Cells and virus

HEK293T (ATCC, #CCL-11268), Vero-E6 (ATCC, #CRL-1586), Huh7 and HeLa cells overexpressing human ACE2 (HeLa-ACE2) were cultured in Dulbecco's Modified Eagle Medium (Gibco) supplemented with 10% fetal bovine serum (Gibco), 1% penicillin-streptomycin (Gibco), and maintained at 37 °C in a humidified atmosphere containing 5% CO_2. SARS-CoV-2 virus was provided by the NIH. Viruses were propagated in Vero-E6 cells and titrated by $TCID_{50}$. Cells were infected with SARS-CoV-2 at the indicated multiplicity of infection (MOI) in Opti-MEM for 1 h and then cultured with fresh medium supplemented with 2% fetal bovine serum. All experiments involving the SARS-CoV-2 virus were performed in the BSL-3 laboratory at the University of California, Los Angeles (UCLA).

2.2. Plasmids and antibodies

SARS-CoV-2 ORF8-FLAG plasmid was kindly provided by Dr. Pei-Hui Wang (Zhang et al., 2020a). HA-tagged recombinant plasmids encoding human SERPINE1, TNFAIP2, IFITM1, and DDX60 were constructed by PCR-based amplification and then subcloned into the pCMV-C-HA eukaryotic expression vector (Beyotime, #D2639). The clones were confirmed by DNA sequencing. Antibodies used for immunoblotting were: Rabbit anti DDDDK-Tag pAb (ABclonal, #AE004), HA-Tag (6E2) mouse mAb (CST, #2367), IRDye 800CW goat anti-mouse IgG (H+L) (LI-COR Biosciences, #925-32210), and IRDye 680LT goat anti-rabbit IgG (H+L) (LI-COR Biosciences, #926-6802).

2.3. SARS-CoV-2-human interactome and network analysis

The SARS-CoV-2-human interactome is composed of two levels of interactions, including SARS-CoV-2-human PPIs and human-human PPIs. The first level (direct SARS-CoV-2-human PPIs) was manually curated from published studies, comprising PPIs data obtained by four experimental methods: affinity purification-mass spectrometry, proximity-dependent biotin labeling, genome-wide yeast-two hybrid (Y2H) screens and co-immunoprecipitations (Co-IP). The second level (SARS-CoV-2 infection associated PPIs) was downloaded from HuRI database (Luck et al., 2020) (www.interactome-atlas.org). The HuRI consists of human-human PPIs screened using high throughput Y2H. Network topology analyses were performed using package igraph version 1.2.6 (https://github.com/igraph) in R (version 3.6.2). The degree function was used to calculate the degree (the total number of a node's neighbors). The betweenness function was employed to calculate the betweenness centrality (the number of shortest paths passing through a node, representing network centrality) (Mao and Zhang, 2013). The function shortest.paths was utilized to calculate the average shortest path length (the average length of all shortest paths from the node to other nodes in the network). The final PPI network was visualized by Cytoscape Version 3.7.2 (Su et al., 2014).

2.4. Transcriptome analysis

Identification datasets were downloaded from GEO database (accession numbers: GSE153970, GSE150392, GSE150819, GSE148729, and GSE147507) and National Genomics Data Center (https://bigd.big.ac.cn/; accession number PRJCA002617 (Sun et al., 2020)). Raw reads were assessed using FASTQC v0.11.9 (https://github.com/s-andrews/FastQC) and trimmed using Trimmomatic v0.38 (Bolger et al., 2014). STAR aligner (v2.7.2a) was performed to map the filtered reads to the human GRCh38 reference genome (Dobin et al., 2013). HTSeq (version 0.9.1) was used to retrieve the raw counts for each gene (Anders et al., 2015) and the differential expression genes (DEGs) were calculated by R package DEseq2 (Love et al., 2014) (with P-value < 0.01, $|\log_2 FC| \geq 1$). The R package RobustRankAggreg (RRA) (Kolde et al., 2012) was applied to identify CLCGs in multiple cell lines infected by SARS-CoV-2 (with adjust P-value < 0.05, $|\log_2 FC| \geq 1$). This RRA method assumes that each gene in each dataset is randomly arranged. It identifies genes that ranked consistently across multiple cell lines. The validation dataset was a bronchoalveolar lavage fluid (BALF) single-cell RNA sequencing (scRNA-seq) data from GSE145926 (Liao et al., 2020) and was analyzed by R package Seurat version 3.1.4 (Stuart et al., 2019).

2.5. Gene set enrichment analysis

The R package "clusterProfiler" (version 3.14.3) (Yu et al., 2012) was used for functional enrichment analysis. The enrichGO and enrichKEGG function were utilized to query the Gene Ontology (GO) function and Kyoto Encyclopedia of Genes and Genomes (KEGG) pathway, respectively.

2.6. Transcription factors enrichment analysis

Transcription factors enrichment analysis was performed to analyze the enrichment of upstream transcription factors (TFs) based on the overlap between a given gene set and previously annotated TFs targets. ChEA3 (Keenan et al., 2019) was employed as a TFs enrichment analysis tool to predict upstream TFs. TFs targets were assembled from ENCODE ChIP-seq library.

2.7. Knockdown of SERPINE1 using siRNA

siRNAs targeting human *Serpine1* (sc-36179) and negative control siRNA (sc-37007) were purchased from SantaCruz (Dallas, USA). At 12 h after cell seeding, cells were transfected with the siRNAs using INTERFERin (Polyplus, Illkirch-Graffenstaden, France) siRNA transfection reagent according to the manufacturer's instruction. At 24 h after siRNA transfection, cells were collected for interference efficiency detection by RT-qPCR or immunoblotting.

2.8. Immunoblotting

Cells were harvested and lysed in RIPA lysis buffer (50 mmol/L Tris-HCl (pH 7.4), 150 mmol/L NaCl, 0.25% sodium deoxycholate, 1% NP-40, 1 mmol/L EDTA, phosphatase and protease inhibitor cocktails (Roche, Basel, Switzerland)) on ice for 30 min. The supernatant was collected after centrifugation at 13,500 ×*g* for 15 min. Protein concentrations were determined by a BCA protein assay kit (Thermo Fisher Scientific, Waltham, USA). Equal amounts of proteins were loaded to SDS-PAGE and transferred onto polyvinylidene fluoride (PVDF) membrane. The membranes were blocked with 5% (w/v) nonfat milk in TBST (50 mmol/L Tris pH 8.0, 150 mmol/L NaCl, 0.05% Tween-20) buffer, incubated with antibodies and visualized by an Odyssey Clx infrared imager (LI-COR Biosciences, Lincoln, USA).

2.9. Immunoprecipitation

HEK293T cells cultured in 6 cm dishes were transfected with various plasmids. Cells were collected and lysed with RIPA lysis buffer. Supernatants were collected by centrifugation (13,500 ×*g*, 15 min, 4 °C) and incubated with anti-HA or anti-FLAG Magnetic Beads (MedChemExpress, Monmouth Junction, USA) overnight at 4 °C. Beads were washed three times with IP-wash buffer (50 mmol/L Tris-Cl (pH 7.4), 150 mmol/L NaCl, 0.25% sodium deoxycholate, 2% NP-40, 1 mmol/L EDTA). Immunoprecipitated proteins were eluted by heating the beads to 98 °C in 1× SDS-PAGE loading buffer and analyzed by immunoblotting.

2.10. Quantitative real time PCR analysis

Cellular total RNA was isolated from cells using the RNeasy Mini Kit (Qiagen, Hilden, Germany) with on-column digestion of genomic DNA. Viral genome RNA in virus suspension were extracted using PureLink Viral RNA/DNA Mini Kit (Thermo Fisher Scientific, Waltham, USA). The RNAs were reverse transcribed to synthesize cDNA using the PrimeScript™ RT reagent Kit (TaKaRa, Dalian, China) according to the manufacturer's protocol. Quantitative real time PCR was performed using LightCycler 480 SYBR Green I Master mix (Roche, Basel, Switzerland), and the threshold cycle (Ct) values of the samples were measured with a LightCycler 480 (Roche, Basel, Switzerland). cDNA quantities were normalized to GAPDH. All primers used were listed in Supplementary Table S1.

2.11. Confocal immunofluorescence assay

HeLa cell monolayers adhered to coverslips were transfected with the indicated plasmids for 24 h. The cells were washed twice with Phosphate Buffered Saline (PBS), and fixed with 4% paraformaldehyde for 15 min at room temperature. Subsequently, the cells were permeabilized with PBS containing 0.2% Triton X-100 for 30 min at room temperature and blocked with bovine serum albumin (BSA)-PBS solution for 30 min at room temperature. The blocked cells were incubated with the indicated primary antibody (1:500) overnight at 4 °C, followed by incubation with secondary antibody conjugated to Alexa FluorTM488, Alexa FluorTM594 or Alexa FluorTM647 (1:2000) (Jackson ImmunoResearch Inc., West Grove, USA) at room temperature and protected from light for 1 h. 4',6-diamidino-2-phenylindole (DAPI) was added to the slides to stain the nucleus. Finally, the slides were imaged with a Leica SP8 confocal microscope.

2.12. Statistical analysis

Statistical analysis was performed using R studio version 3.6.2 for statistical computing. Experimental data are presented as mean ± SD. Differences were considered statistically significant when *P* values were less than 0.05. "*" denotes significant difference and "ns" for no significance. $*P < 0.05$, $**P < 0.01$, $***P < 0.001$ and $****P < 0.0001$ for all the analysis.

3. Results

3.1. SARS-CoV-2-human interactome construction and global analysis

To better understand the mechanisms of SARS-CoV-2 replication and pathogenesis at the cellular level, we constructed and analyzed the virus-host interactome. The SARS-CoV-2-human interactome consists of two levels of interactions: PPIs between SARS-CoV-2 and human proteins, and PPIs among human proteins. Firstly, we curated direct interactions between SARS-CoV-2 and human proteins from published studies (Supplementary Table S2). The results showed that 31 viral proteins encoded by SARS-CoV-2 could directly interact with 3591 human proteins, which were defined as SARS-CoV-2 directly interacting human proteins (SIPs). These SIPs interacted with at least one SARS-CoV-2 protein, and some of them can interact with multiple viral proteins simultaneously, resulting in 11,755 interacting pairs (Fig. 1A). To gain insight into virus-induced perturbations and the function of SIPs in the human host, we then mapped the network onto a human PPIs network (HuRI). We identified 3848 human interactors of 1459 SIPs in HuRI and yielded 16,694 non-redundant PPIs between these 5307 human proteins. The 3848 human interactors of SIPs were defined as SARS-CoV-2 infection associated human proteins (SAPs). Finally, we constructed a large SARS-CoV-2-human protein interactome consisting of SARS-CoV-2 viral proteins, SIPs and SAPs, with 7470 nodes and 28,449 non-redundant edges (Fig. 1A).

Previous studies have showed that virus directly interacting proteins usually play a central role in the host PPIs network, and targeting these proteins may seriously affect the balance of the host network (Perrin--Cocon et al., 2020; Zhang et al., 2021b). In order to provide novel insights into virus-host interactions, the degree, betweenness centrality and average shortest path length were calculated for each protein in HuRI. SIPs had a median degree, betweenness centrality, and average shortest path length of 4, 2 and 3.8, respectively, compared to 9, 286.3 and 3.6 for SAPs and 2, 0, and 4 for all other human proteins in HuRI (Fig. 1B). SIPs and SAPs showed higher betweenness centrality and degree, as well as smaller average shortest path length when compared to other human proteins (student's *t*-test, $P < 0.01$). This suggests that SIPs and SAPs exert a substantial effect on human interactome. Additionally, the degree distributions of each viral protein and human protein were investigated. The top five viral proteins were ORF7b, M, NSP6, NSP4, and ORF7a (Fig. 1C). As a viral attenuation factor in SARS-CoV (Pfefferle et al., 2009), ORF7b had the highest degree. ORF8 ranked seventh and has been reported to function in immune evasion during SARS-CoV-2 infection (Zhang et al., 2021a). In the top 30 human protein degree distributions, 29 out of the top 30 proteins were SIPs that directly interacted with viral proteins (Fig. 1C).

Next, we performed GO enrichment analysis for SIPs of each viral protein. Research indicated that the localization of interaction partners is somewhat consistent with the localization of viral proteins, and the cellular component enrichment can convey important information regarding function (Gordon et al., 2020b). Consistent with previous study (Gordon et al., 2020b), cellular component enrichment showed that SIPs of a variety of SARS-CoV-2 NSPs were mainly located in the cytoplasm: NSP1 and NSP8 interactors were significantly enriched in

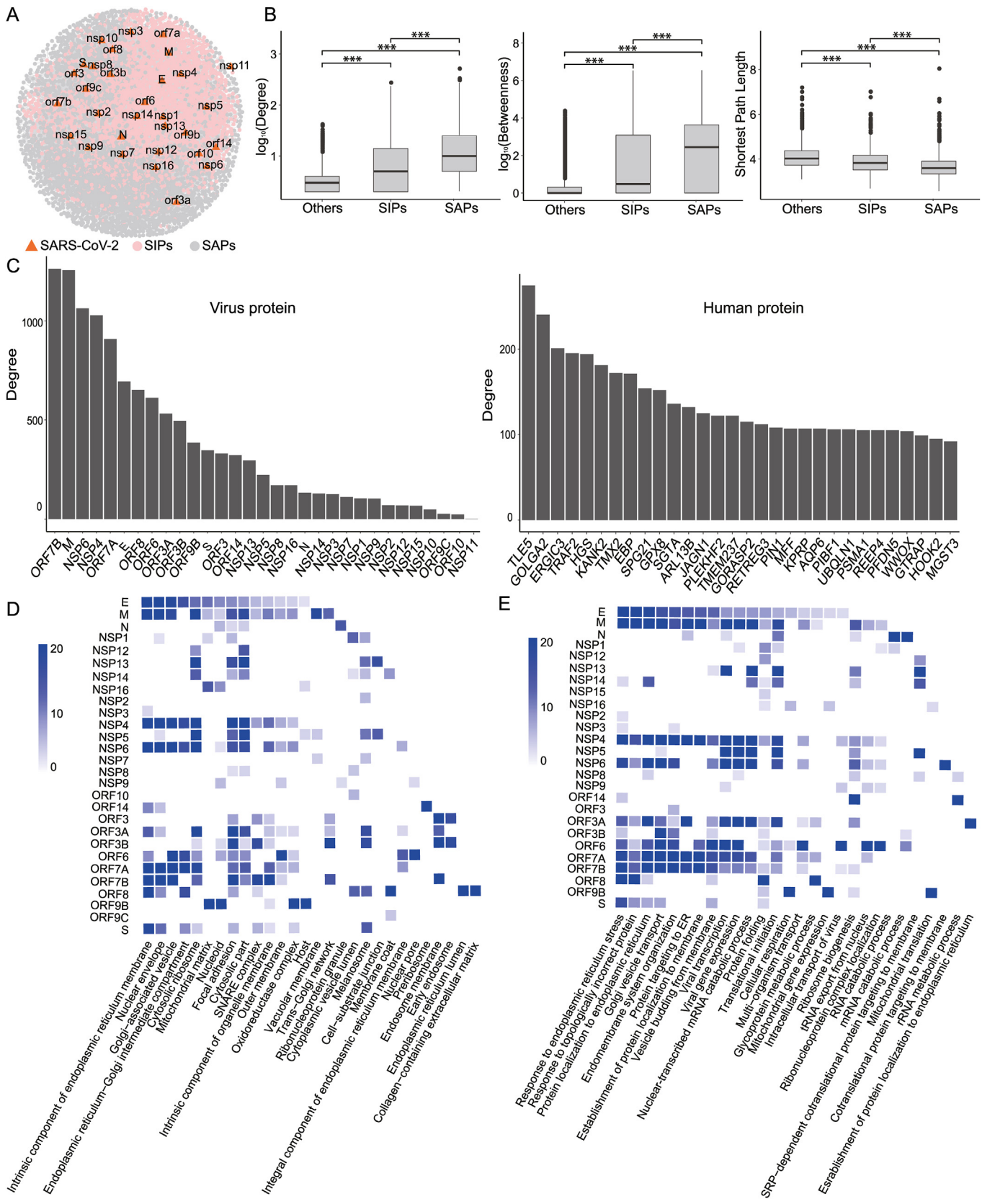

Fig. 1. Global analysis of the SARS-CoV-2-human interactome. **A** The SARS-CoV-2 interactome includes 7470 nodes and 28,449 non-redundant edges. Orange triangles represent SARS-CoV-2 viral proteins, pink circles represent SARS-CoV-2 directly interacting human proteins (SIPs), and gray circles represent human interactors of SIPs (SAPs). **B** Distribution of degree, betweenness centrality, and shortest path length for SIPs, SAPs and other human proteins in the human protein-protein interaction network (HuRI). **C** Degree distribution of SARS-CoV-2 viral proteins and top 30 human proteins. **D** Cellular component enrichment and (**E**) biological process enrichment of SIPs for each viral protein. Color indicates $-\log_{10}$(p.adjust).

"cytoplasmic vesicle lumen", while NSP5, NSP12, NSP13 and NSP14 interactors were predominantly enriched in "cytosolic ribosome" and "cytosolic part". In addition to cytoplasm related terms, SIPs of NSP4 and NSP6 were also significantly enriched in ER related GO terms. NSP9 interactors were primarily found in nuclear related terms, such as "nuclear pore" and "nucleoid". The interactors of accessory protein ORF8 were mostly enriched in ER related terms: "intrinsic component of endoplasmic reticulum membrane", "endoplasmic reticulum-Golgi intermediate compartment", "integral component of endoplasmic reticulum membrane" and "endoplasmic reticulum lumen" (Fig. 1D and Supplementary Table S3). In agreement with cellular component enrichment result, the biological process enrichment analysis of ORF8 interactors was also mainly associated with ER related pathways such as "response to endoplasmic reticulum stress", "response to topologically incorrect protein", "protein localization to endoplasmic reticulum", and "protein folding" (Fig. 1E). Furthermore, we found that the SIPs corresponding to each viral protein were generally enriched in multiple GO terms (Fig. 1E and Supplementary Table S4), indicating the complexity of virus-affected perturbations of the host biological network.

3.2. Identification of multiple cell lines common genes (CLCGs) in SARS-CoV-2 infection

In the past few years, a large number of studies have investigated transcriptome changes in host cells caused by SARS-CoV-2 infection (Wang et al., 2021; Li et al., 2022). These transcriptomics studies have greatly helped us to understand the pathogenesis and immune mechanisms of SARS-CoV-2. To further mine more important information about the host cell response to SARS-CoV-2 infection, we reanalyzed the DEGs of six different datasets (Supplementary Table S5) by the DESeq2 package. The datasets we used include data from various cell lines, sequencing platforms, infection time, and multiplicities of infection. We found that DEGs overlap among different cell lines varies significantly, and considerable variation also presented in the same cell line with different infection time or multiplicity of infection (Fig. 2A), indicating that these cell lines can flexibly respond to SARS-CoV-2 infection in a cell-specific manner. Given the huge disparity in transcriptome changes among multiple cell lines, we used the R package RRA to identify DEGs with consistent changes in multiple cell lines infected by SARS-CoV-2. Through rank analysis, we identified 123 CLCGs in all cell lines, including 115 up-regulated genes and 8 down-regulated genes (Fig. 2B).

We found that most of the up-regulated CLCGs in virus-infected cells were genes related to cellular innate immunity, including interferon genes (e.g., IFNB1, IFNL3, IFNL1, IFNL2) and interferon stimulated genes (ISGs) (e.g., MX1, CH25H, OASL, etc.). In addition, SARS-CoV-2 infection also induced robust expression of chemokines and inflammatory cytokine genes, such as CXCL2, CCL20, IL1A, IL6, TNF, TNFRSF9, etc. (Fig. 2B). Meanwhile, functional enrichment analysis of the CLCGs revealed that they were mainly involved in type I interferon signaling pathway, regulation of cytokine production, and leukocyte chemotaxis. In addition to significant enrichment in the term “Coronavirus disease-COVID-19”, many other viruses related pathways were also enriched by KEGG enrichment analysis, such as Influenza A, Epstein-Barr virus, Hepatitis C, etc. (Fig. 2C and Supplementary Table S6), suggesting that CLCGs may be universally up-regulated genes following viral infection. To determine whether CLCGs were still differentially expressed at the patient level, we next validated the expression of CLCGs in BALF epithelial cells from COVID-19 patients. The results showed that most of the up-regulated CLCGs remained upregulated in epithelial cells from patients with moderate or severe COVID-19 compared to healthy individuals (Fig. 2D).

3.3. Identification of key host factors interacting with SARS-CoV-2

Based on the aforementioned systematic analysis of SARS-CoV-2-human interactome and CLCGs, we aimed to identify core host genes that were critical for SARS-CoV-2 infection and pathogenesis. We first overlapped the SARS-CoV-2-human interactome with the CLCGs, and obtained 35 core host genes, as showed in Fig. 3A and Supplementary Table S7. Then, the biological functions of these 35 core host genes were annotated through the Metascape website. The resulting network revealed that the core host genes were linked to "response to virus", "response to interferon-beta", "TNF signaling pathway" and "regulation of cytokine production involved in immune" (Fig. 3B). The enrichment of each CLCG in different signaling pathways was shown in the heatmap of Fig. 3C. We found that the majority of core host genes were enriched in more than one signaling pathway, with TNF signaling pathway, regulation of cytokine production, and regulation of defense response related terms being significantly enriched by multiple core host genes.

To narrow down the list of candidate genes, co-expression and network analysis was performed. Co-expression analysis can identify genes that have coordinated expression patterns and may be functionally related. The time-series data (PRJCA002617) was used for co-expression analysis of the 35 core host genes. After clustering the Pearson's correlation coefficient (PCC) matrix of all core host genes, we found that the up-regulated and down-regulated genes showed strong co-expression, respectively (Fig. 3D). Among the up-regulated genes, SERPINE1, TNFAIP2 and RND1 formed a strongly related co-expressed gene module, while BATF2, OAS1 and XAF1 also formed a co-expressed gene module. Additionally, the remaining 25 genes showed a high positive correlation in expression. To learn more about these 35 core host genes and their function, the functional protein association networks STRING (https://cn.string-db.org) was used to construct the co-expression network. 23 out of 31 up-regulated core host genes had inner interactions (Fig. 3E). Mapping the time-series data to the network, we found that 16 genes were up-regulated at 0 h post-infection (hpi), 10 genes at 7 hpi, 21 genes at 12 hpi, and 22 genes at 24 hpi, respectively. It indicated that the host elicited a complicated response in the very early stage of SARS-CoV-2 infection, and the response become stronger over time. The host up-regulates immune-related genes to defend against SARS-CoV-2 infection, meanwhile, the virus employs various strategies to manipulate host factors in favor of its own survival.

To recognize significant transcriptional changes and get insights into the transcriptional machinery, we employed ChEA3 database to decode the upstream TFs. We predicted 26 TFs (FET P-value <0.05) from the ENCODE ChIP-seq library to regulate the co-expression network (Supplementary Fig. S1 and Supplementary Table S8). STAT2 and STAT1 had the most significant P-values, while HNF4A regulated the greatest number of genes in the co-expression network. Several studies have revealed that SARS-CoV-2 N protein can block STAT1/STAT2 phosphorylation or nuclear translocation to antagonize IFN-I signaling (Mu et al., 2020; Xia et al., 2020). Furthermore, STAT2 may be involved in restricting virus dissemination (Boudewijns et al., 2020). Finally, we selected four SIPs (SERPINE1, TNFAIP2, IFITM1 and DDX60) in the co-expression network that directly interact with SARS-CoV-2 as key host factors for further study (Fig. 3F).

3.4. In vitro confirmation of the key host factors

Next, we verified the direct interactions between above identified key host factors (SERPINE1, TNFAIP2, IFITM1 and DDX60) and corresponding viral proteins. We cloned these human genes and SARS-CoV-2 viral protein expression sequences into HA or Flag-tagged expression vectors and tested the interaction by co-immunoprecipitation assay. The results showed successful detection of interactions between all four key host factors and SARS-CoV-2 viral proteins. TNFAIP2 was able to interact with viral proteins ORF7b, NSP4, and M. IFITM1 can interact with ORF7b and ORF3. DDX60 can interact with NSP1 (Supplementary Fig. S2A), and the interaction between SERPINE1 and ORF8 was readily detectable in reciprocal immunoprecipitation experiments (Fig. 4A).

Using a time-series dataset (PRJCA002617), we then assessed the dynamic expression of the four key host genes during SARS-CoV-2 infection (Supplementary Fig. S2B). SERPINE1 and TNFAIP2 were

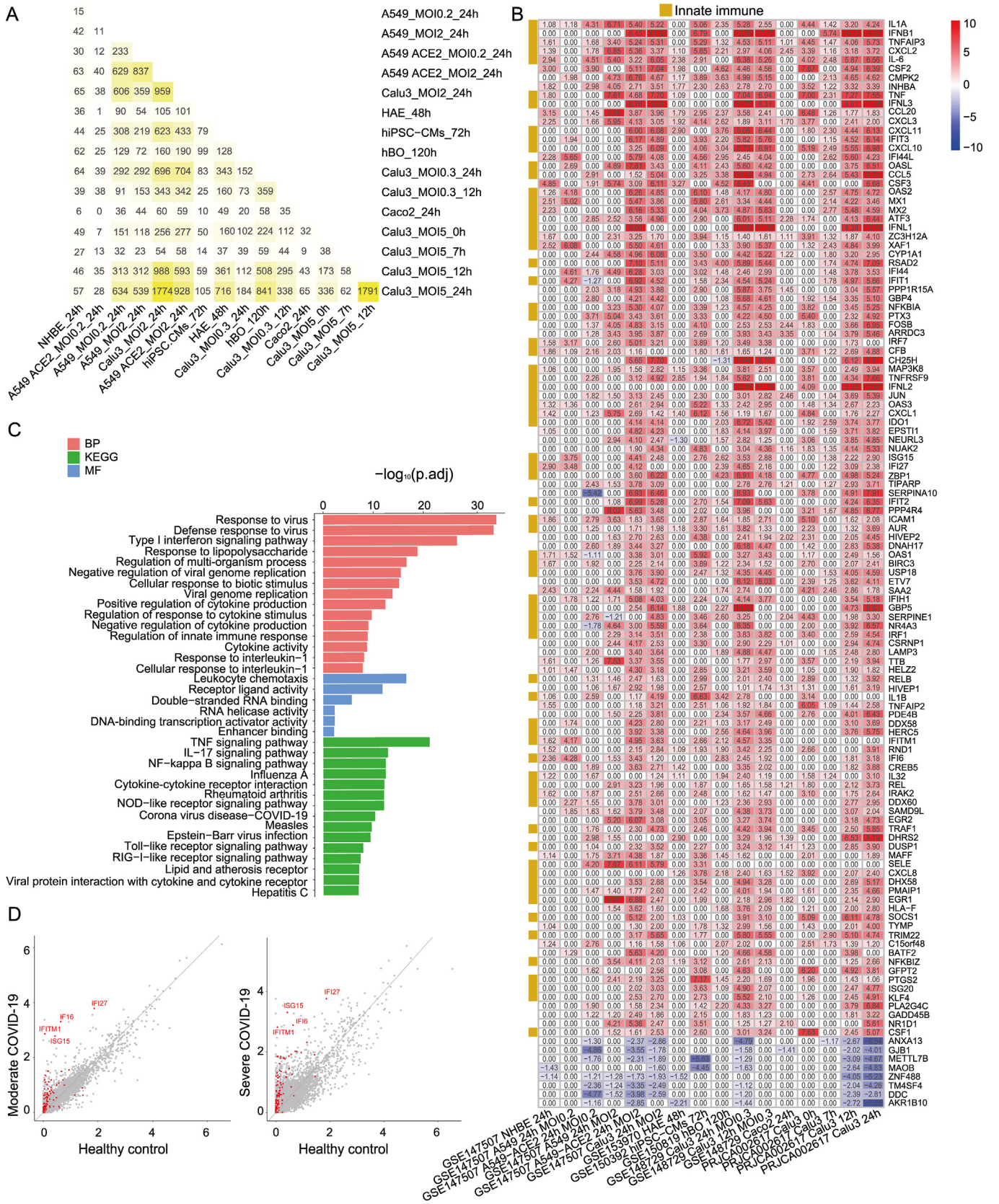

Fig. 2. Systematic analysis of the transcriptome of multiple cell lines infected by SARS-CoV-2. **A** Overlap of differentially expressed genes (DEGs, p.adjust < 0.01, $|\log_2 FC| \geq 1$) in multiple cell lines with SARS-CoV-2 infection. **B** Log_2FC heatmap of CLCGs in multiple cell lines infected with SARS-CoV-2. **C** GO and KEGG analysis of CLCGs. **D** CLCGs expression in BALF-derived epithelial cells in patients with moderate (left) and severe/critical (right) infection.

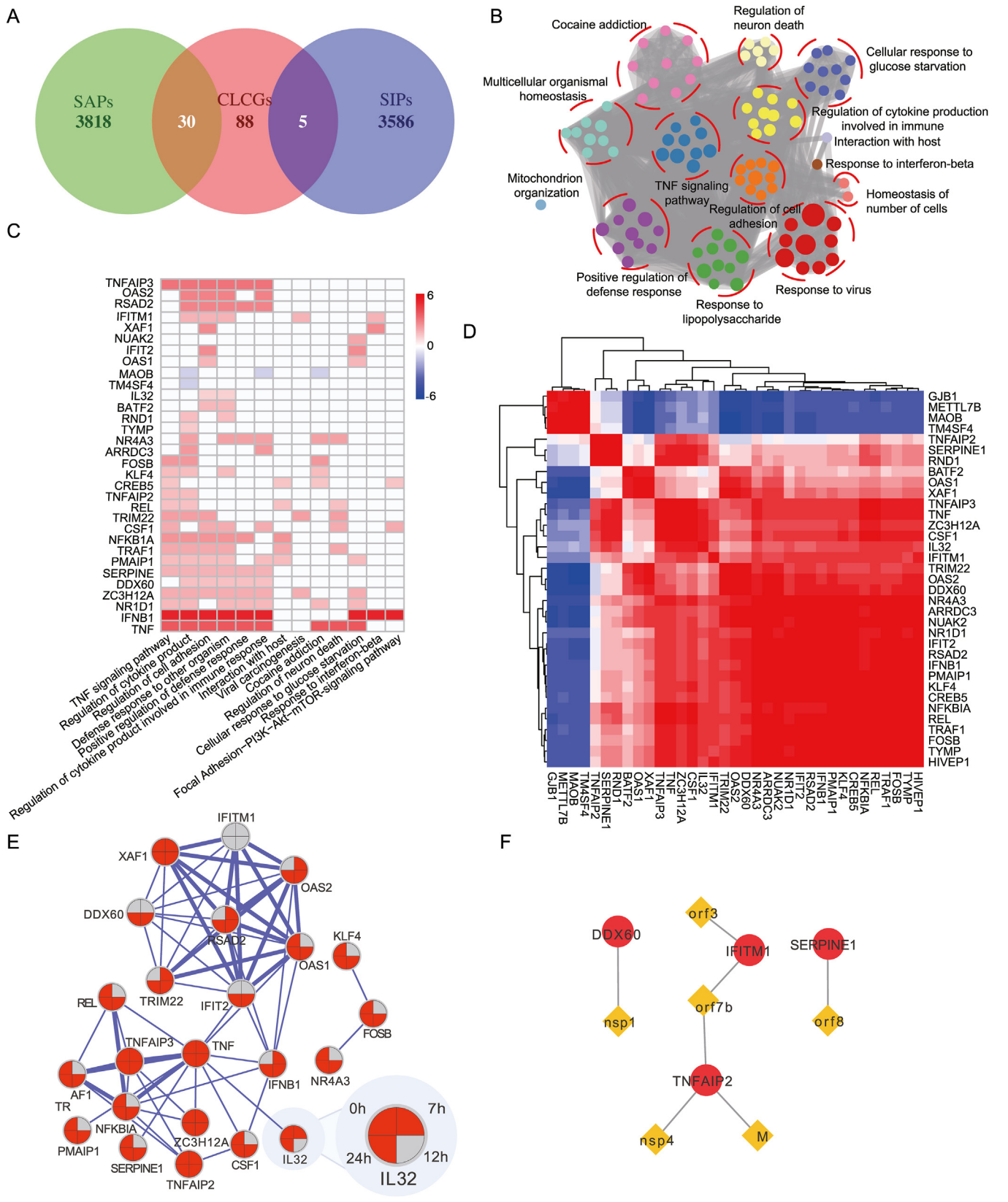

Fig. 3. Identification of key host factors interacting with SARS-CoV-2. **A** Venn diagram of CLCGs with SIPs and SAPs. 35 overlapped genes are defined as core genes. **B** Network of enriched terms of 35 core genes, where each node represents an enriched term and is colored by its cluster ID. **C** Heatmap of each core gene participated pathways. **D** Co-expression of 35 core genes, where red indicates a positive correlation; blue indicates a negative correlation. **E** Co-expression network. Each node stands for a core gene. For each node, the top left represents gene expression at 0 hpi of SARS-CoV-2 infection, while the top right represents 7 hpi, the bottom right represents 12 hpi, the bottom left represents 24 hpi. Red represents up-regulated (P.adj < 0.01, $|\log_2 FC| > 1$). **F** Interactions of four key host factors with SARS-CoV-2 viral proteins.

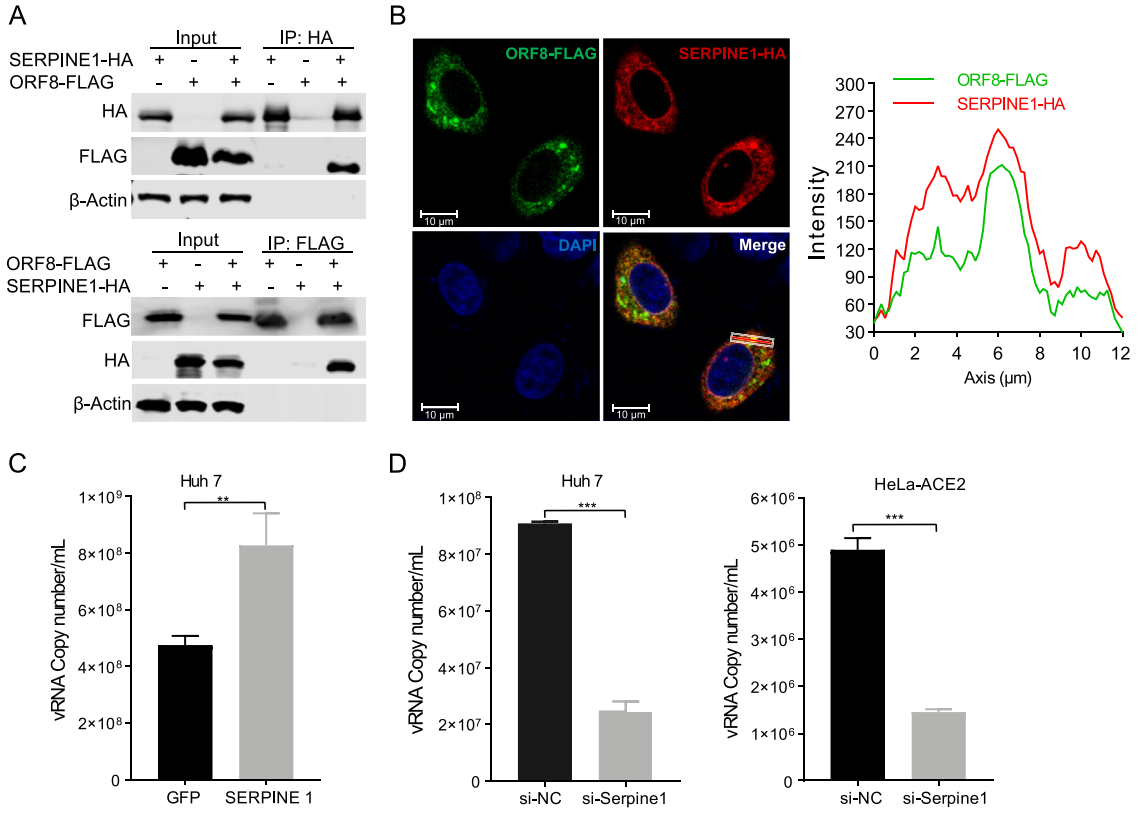

Fig. 4. SERPINE1 interacts with ORF8 and facilitates viral replication. **A** Co-immunoprecipitation of SERPINE1 and ORF8 in HEK 293T cells expressing SERPINE1-HA and ORF8-FLAG. **B** Co-localization analysis of SERPINE1 and ORF8 in HeLa cells expressing SERPINE1-HA and ORF8-FLAG by confocal microscopy. Scale bar, 10 μm. **C** Determination of SARS-CoV-2 genome RNA (vRNA) copies in the supernatant of GFP or SERPINE1 overexpressing cells by real-time PCR assay. **D** Huh7 or HeLa-ACE2 cells were transfected with siRNA against *Serpine1* for 48 h and then infected with SARS-CoV-2 virus at an MOI of 0.01 and incubated for 24 h. The vRNA copies of SARS-CoV-2 in the cell supernatant were determined by real-time PCR assay. Statistical analyses were performed using a two-tailed Student's *t*-test. "*" denotes significant difference. $^{**}P < 0.01$, $^{***}P < 0.001$. Data in (**A**) and (**B**) were representatives of three independent experiments, data in (**C**) and (**D**) were shown as mean ± SD of three independent experiments.

considerably up-regulated in Calu-3 cells during the early SARS-CoV-2 infection (0 hpi). DDX60 exhibited persistent up-regulation following SARS-CoV-2 infection. Although IFITM1 appeared to be up-regulated, it was not statistically significant (*P*-value > 0.01). To validate the expression of the four key host factors, quantitative analysis by RT-qPCR was performed. The result showed that four genes were significantly elevated after SARS-CoV-2 infection (Supplementary Fig. S2C). The expression patterns of SERPINE1, DDX60 and TNFAIP2 exhibited high consistencies with those of RNA-Seq results (Supplementary Fig. S2B), whereas IFITM1 displayed continuous up-regulation from 7 hpi.

3.5. SERPINE1, an ORF8 interacting protein, facilitates SARS-CoV-2 replication

To demonstrate the experimental value of the identified key host factors, we focused on SERPINE1 and conducted further studies. The interactome analysis and co-immunoprecipitation experiments showed a clear and strong interaction between SERPINE1 and ORF8 (Fig. 4A). We further examined their subcellular localization in co-expression cells. As shown in Fig. 4B, ORF8 and SERPINE1 were all present predominately in the cytoplasm and co-localized to form punctate bodies. To further study the role of SERPINE1 in SARS-CoV-2 infection, Huh7 cells were transfected with GFP or HA-tagged SERPINE1 expression plasmid, then the transfected cells were infected with SARS-CoV-2. At 48 hpi, the viral genomic RNA copy number in the supernatants was examined by RT-qPCR. The results showed that SARS-CoV-2 replicated more effectively in SERPINE1-overexpressing cells than in GFP-expressing cells (Fig. 4C). Secondly, we treated Huh7 and HeLa-ACE2 cells with *Serpine1* siRNA to knock down *Serpine1* and detected the replication of SARS-CoV-2 in *Serpine1* knockdown cells. Result revealed that the viral growth is remarkably reduced in *Serpine1*-knockdown Huh7 and HeLa-ACE2 cells (Fig. 4D). Taken together, these results indicated that SERPINE1 is a co-host factor that facilitates SARS-CoV-2 replication.

3.6. SERPINE1 alleviates ORF8 mediated ER stress

Considering the importance of the ORF8 interacting protein SERPINE1 for viral replication, we ought to find out the influence of SERPINE1 on the function of ORF8. According to our above integrated analysis, 652 host genes were found to interact with ORF8. These genes were localized primarily in the ER of host cells (Fig. 1D), and were mainly involved in cellular ER stress, unfolded protein response (UPR), and glycoprotein metabolic process via GO analysis (Fig. 1E). In addition, Liu P et al. has reported that ORF8 could induce ER stress through targeting key UPR components (Liu et al., 2022). Consequently, we hypothesized that SERPINE1 may affect ORF8-mediated ER stress. To test this hypothesis, we first examined whether the interaction between SERPINE1 and ORF8 occurred in ER. In cells expressing SERPINE1-HA, ORF8-FLAG and ER tracker ER-DsRed2, we found that SERPINE1-HA and ORF8-FLAG were co-localized in the ER-DSRED2-labeled ER (Fig. 5A). Then, we

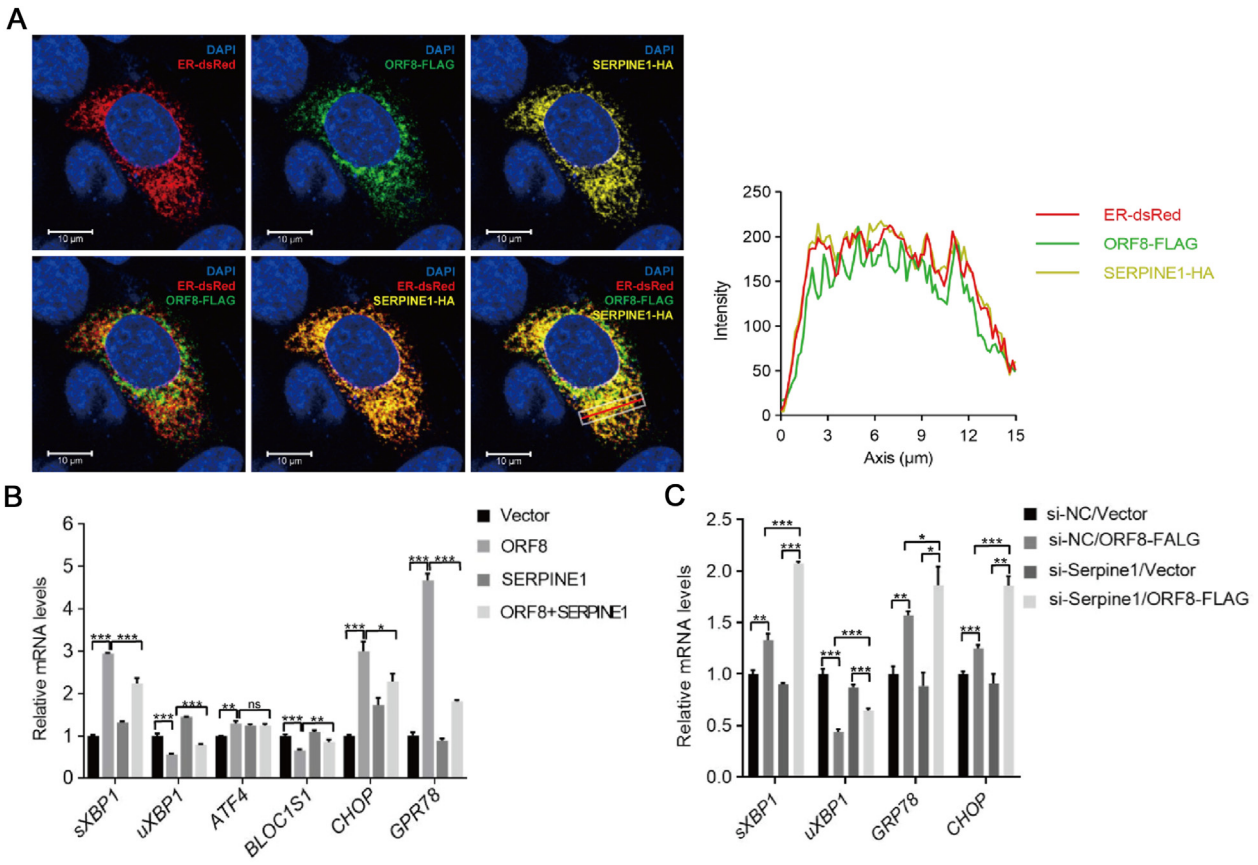

Fig. 5. SERPINE1 can alleviate ER stress induced by ORF8. **A** Co-localization of ERp72-dsRed (ER-dsRed), ORF8-FLAG (green), and SERPINE1-HA (yellow) in HeLa cells, nuclei were stained with DAPI (blue). Scale bars, 10 μm. Images shown were representatives of three independent experiments. **B** Detection of featured gene (uXBP1, sXBP1, ATF4, BLOC1S1, CHOP and GRP78) expression of ER stress by real-time PCR in HEK 293T cells expressing ORF8-FLAG, SERPINE1-HA or the combination of ORF8-FLAG and SERPINE1-HA. **C** Detection of ORF8 induced uXBP1, sXBP1, CHOP and GRP78 mRNA levels by real-time PCR in HEK 293T cells transfected with scrambled control siRNA (siNC) or siRNA against *Serpine1*. Real-time PCR data were presented as mean ± SD. Statistical analyses were performed using a two-tailed Student's *t*-test. "*" denotes significant difference and "ns" for no significance. $^{*}P < 0.05$, $^{**}P < 0.01$ and $^{***}P < 0.001$.

examined the ORF8-induced ER stress in SERPINE1 overexpressing cells and knockdown cells, respectively. As shown in Fig. 5B, the expression of ER stress characteristic genes was easily detected in ORF8 overexpressing cells, including upregulated mRNA level of spliced XBP1 (sXBP1), ATF4, CHOP, GPR78 and downregulation of un-spliced XBP1 (uXBP1) and BLOC1S1, but these were reversed in cells overexpressing SERPINE1. However, in *Serpine1* knockdown cells, ORF8 mediated stronger ER stress than in control cells (Fig. 5C). These results suggested that SERPINE1 could alleviate the ER stress induced by ORF8 protein.

4. Discussion

The COVID-19 pandemic has caused a devastating impact across the whole world. The pathogenesis of SARS-CoV-2 is complicated and poorly understood. Evidence showed that both viral and host factors play key roles in COVID-19, affecting the disease course in a complex manner (Zhang et al., 2020b). Gene expression studies and interactome analysis have been widely used in COVID-19 study (Chakraborty et al., 2021; Mahmud et al., 2021). Given the massive dimensions and diversity of available data, omics-scale integration analyses will provide an enormous opportunity to better understand the pathobiology complexities of COVID-19, as well as provide novel insights into potential therapeutic targets (Li et al., 2022). This study employed a systematic integrated analysis of SARS-CoV-2 transcriptome and interactome, aiming to explore general characteristics and identify crucial genes in SARS-CoV-2 infection through this unbiased data-driven approach.

By searching literature and database, we constructed a comprehensive SARS-CoV-2-human interactome. The entry of virus into host cells resulted in a complex network of interactions. Deciphering the interplay between SARS-CoV-2 and the host is of primary importance in the study of virus life cycle and host defense response (Terracciano et al., 2021). From a systems biology point of view, we found that SIPs and SAPs played vital roles in the human networks (Fig. 1B), indicating that targeting these genes may affect the homeostasis of human networks. Consistent with results from Gordon D.E. et al. (Gordon et al., 2020a), the SIPs corresponding to each viral protein were involved in a number of essential cellular pathways (Fig. 1D), including host antiviral immune response and a number of pathways that conducive to the viral exploitation of host resources. In order to screen vital genes closely related to SARS-CoV-2 infection, transcriptome expression data was included in the analysis. Transcriptome analysis after viral infection can facilitate understanding the dynamic response of host immunity and identification important host factors (Fagone et al., 2020). The approach we employed is significantly different from previous single SARS-CoV-2 transcriptome study because the results obtained by single sequencing data cannot be well verified in other data generated by different laboratories and the results from different cell lines have internal heterogeneity. To detect core genes more accurately, we performed a robust RRA approach based on gene ranking across eight cell lines. 115 up-regulated CLCGs and 8 down-regulated CLCGs were identified. In agreement with the findings of others (Blanco-Melo et al., 2020a), transcriptomic profiling revealed robust levels of IFN, inflammatory cytokines and chemokines, suggesting

the signature of elevated innate immunity and "cytokine storm" induced by SARS-CoV-2 (Hu et al., 2021; Ramasamy and Subbian, 2021).

Through co-expression, network analysis and experimental confirmation of immunoprecipitation, four genes in the co-expression network, including IFITM1, SERPINE1, DDX60 and TNFAIP2, were found to directly interact with SARS-CoV-2 viral proteins and were thought to be key host factors during SARS-CoV-2 infection. Some of these genes have been proved to play special roles in SARS-CoV-2 infection. As an IFN-induced transmembrane protein, IFITM1 was shown to mechanically alter membrane lipid order and curvature to limit viral-cell fusion and thereby impede virus infection at the entry stage (Huang et al., 2011; Wrensch et al., 2014). Evidence showed that IFITM1 were strongly up-regulated during the innate immune response in COVID-19 patients (Blanco-Melo et al., 2020a; Hadjadj et al., 2020). Interestingly, IFITM1 has been revealed to have dual function roles, promoting (Prelli Bozzo et al., 2021) or inhibiting (Buchrieser et al., 2020; Shi et al., 2021) SARS-CoV-2 infection depending on the experimental settings and cell types. Although IFITM1 is best known for its antiviral activity, its additional physiological functions in SARS-CoV-2 infection merit further investigation. DDX60 was discovered to be a ligand-specific sentinel for RIG-I activation and is involved in the viral RNA degradation process (Miyashita et al., 2011; Oshiumi et al., 2015). TNFAIP2 is associated with autoimmune diseases (Jia et al., 2018) and may be involved in antiviral responses (Chevrier et al., 2011), but its role in coronavirus remains unknown and merits in-depth mechanistic study.

SERPINE1, encoding plasminogen activator inhibitor 1 (PAI-1), is a member of the SERPIN superfamily and one of the key host factors that can interact with the viral ORF8 protein. In this study, we found that the expression of SERPINE1 was elevated in multiple cell lines. Several studies also shown that SERPINE1 was over-expressed in plasma (Goshua et al., 2020; Zuo et al., 2021) and lungs (Ackermann et al., 2020) of COVID-19 patients. Dittmann M. et al. had reported that PAI-1 could block the maturation of progeny influenza A virus (IAV) particles by targeting extracellular airway proteases and inhibit IAV glycoprotein cleavage (Dittmann et al., 2015). In addition, we noticed that SERPINA1, another important member of the SERPIN family, could suppress SARS-CoV-2 replication in cell lines and primary cells by binding and inactivating the serine protease TMPRSS2 (Wettstein et al., 2021). In contrast to its antiviral activity in IAV and the function of SERPINA1 in SARS-CoV-2, our study showed that SERPINE1 facilitated SARS-CoV-2 replication in cells. This reflects the complexity and uniqueness of the interaction between SARS-CoV-2 and the host factors. Given the fact that 652 ORF8 interacting host proteins were mainly localized in ER and engaged in cellular ER stress, UPR, and glycoprotein metabolic process (Fig. 1D and E), and the fact that ORF8 has been reported to induce ER stress and regulate ER reshaping (Liu et al., 2022), our following study focused on the effect of SERPINE1 on ORF8 function. The result showed that SERPINE1 interacted with ORF8, could alleviate the ORF8-induced ER stress. It was known that viruses rely entirely on host cell to synthesize and fold viral proteins. During viral replication, the sudden need to process large amounts of viral glycoproteins drive the ER beyond its physiological ability to fold proteins and will lead to ER stress. However, unresolved or excessive ER stress drives host cells into apoptosis (Galluzzi et al., 2008; Sano and Reed, 2013). It has been shown that viruses use various strategies to balance ER stress. Herpes simplex virus 1 UL41 protein can suppresses the IRE1/XBP1 signal pathway of the UPR via its endoribonuclease activity (Zhang et al., 2017). IAV relieves ER stress by NS1 interfering with the host messenger RNA processing factor CPSF30 and suppressing ER stress response factors to benefit IAV replication (Mazel-Sanchez et al., 2021). Thus, we speculate that SARS-CoV-2 may trickily utilize SERPINE1 to balance the ER stress caused by ORF8, thereby limiting the inevitable ER stress to a beneficial level for SARS-CoV-2 replication. However, the underlying mechanism remains unclear and requires further study.

5. Conclusions

In conclusion, our findings provide a comprehensive perspective of virus-host interactions of SARS-CoV-2. Based on the integrated analysis of SARS-CoV-2 interactome and transcriptome, four key host genes (IFITM1, SERPINE1, DDX60, and TNFAIP2) were identified as candidates that may be involved in SARS-CoV-2 infection. Furthermore, one of the identified genes, SERPINE1 was found to interact with the SARS-CoV-2 ORF8 protein and could alleviate the ER stress induced by the ORF8 protein to benefit SARS-CoV-2 replication. This study highlights the value of multi-omics integration and provides insights for future research on potential therapeutic targets against SARS-CoV-2.

Data availability

The SARS-CoV-2-human PPIs were summarized in Supplementary Table S2. The transcriptome data we used was summarized in Supplementary Table S5.

Ethics statement

This article does not contain any studies with human or animal subjects performed by any of the authors.

Author contributions

Jie Sheng: formal analysis, investigation, data curation, methodology, writing-original draft, writing-review and editing. Lili Li: methodology, data validation, writing-review and editing. Xueying Lv: editing. Meiling Gao: data validation. Ziyi Chen: investigation and data curation. Zhuo Zhou: editing. Jingfeng Wang: data validation, methodology, writing-original draft, writing-review and editing. Aiping Wu: conceptualization and editing. Taijiao Jiang: conceptualization, funding acquisition, resources, supervision, writing-review and editing.

Conflict of interest

The authors declare that they have no conflict of interest.

Acknowledgements

This work was supported by the National Natural Science Foundation of China (32070678, 82102371 and 31671371); the Emergency Key Program of Guangzhou Laboratory, grant no. EKPG21-12; the Self-supporting Program of Guangzhou Laboratory, Grant No. SRPG22-007, SRPG22-020; the National Key Research and Development Program of China (2020YFC0840800); CAMS Innovation Fund for Medical Sciences (CIFMS) (2021-I2M-1-061); the National Key Research and Development Program of China (2021YFC2302000).

Appendix A. Supplementary data

Supplementary data to this article can be found online at https://doi.org/10.1016/j.virs.2023.05.004.

References

Ackermann, M., Verleden, S.E., Kuehnel, M., Haverich, A., Welte, T., Laenger, F., Vanstapel, A., Werlein, C., Stark, H., Tzankov, A., Li, W.W., Li, V.W., Mentzer, S.J., Jonigk, D., 2020. Pulmonary vascular endothelialitis, thrombosis, and angiogenesis in covid-19. N. Engl. J. Med. 383, 120–128.

Aevermann, B.D., Pickett, B.E., Kumar, S., Klem, E.B., Agnihothram, S., Askovich, P.S., Bankhead 3rd, A., Bolles, M., Carter, V., Chang, J., Clauss, T.R., Dash, P., Diercks, A.H., Eisfeld, A.J., Ellis, A., Fan, S., Ferris, M.T., Gralinski, L.E., Green, R.R., Gritsenko, M.A., Hatta, M., Heegel, R.A., Jacobs, J.M., Jeng, S., Josset, L., Kaiser, S.M., Kelly, S., Law, G.L., Li, C., Li, J., Long, C., Luna, M.L., Matzke, M., McDermott, J., Menachery, V., Metz, T.O., Mitchell, H., Monroe, M.E., Navarro, G., Neumann, G., Podyminogin, R.L., Purvine, S.O., Rosenberger, C.M., Sanders, C.J.,

Schepmoes, A.A., Shukla, A.K., Sims, A., Sova, P., Tam, V.C., Tchitchek, N., Thomas, P.G., Tilton, S.C., Totura, A., Wang, J., Webb-Robertson, B.J., Wen, J., Weiss, J.M., Yang, F., Yount, B., Zhang, Q., McWeeney, S., Smith, R.D., Waters, K.M., Kawaoka, Y., Baric, R., Aderem, A., Katze, M.G., Scheuermann, R.H., 2014. A comprehensive collection of systems biology data characterizing the host response to viral infection. Sci. Data 1, 140033.

Anders, S., Pyl, P.T., Huber, W., 2015. Htseq – a python framework to work with high-throughput sequencing data. Bioinformatics 31, 166–169.

Araf, Y., Akter, F., Tang, Y.D., Fatemi, R., Parvez, M.S.A., Zheng, C., Hossain, M.G., 2022. Omicron variant of sars-cov-2: genomics, transmissibility, and responses to current covid-19 vaccines. J. Med. Virol. 94, 1825–1832.

Blanco-Melo, D., Nilsson-Payant, B.E., Liu, W.C., Uhl, S., Hoagland, D., Møller, R., Jordan, T.X., Oishi, K., Panis, M., Sachs, D., Wang, T.T., Schwartz, R.E., Lim, J.K., Albrecht, R.A., tenOever, B.R., 2020a. Imbalanced host response to sars-cov-2 drives development of covid-19. Cell 181, 1036–1045.e1039.

Blanco-Melo, D., Nilsson-Payant, B.E., Liu, W.-C., Uhl, S., Hoagland, D., Møller, R., Jordan, T.X., Oishi, K., Panis, M., Sachs, D., Wang, T.T., Schwartz, R.E., Lim, J.K., Albrecht, R.A., tenOever, B.R., 2020b. Imbalanced host response to sars-cov-2 drives development of covid-19. Cell 181, 1036–1045.e1039.

Bolger, A.M., Lohse, M., Usadel, B., 2014. Trimmomatic: a flexible trimmer for illumina sequence data. Bioinformatics 30, 2114–2120.

Boudewijns, R., Thibaut, H.J., Kaptein, S.J.F., Li, R., Vergote, V., Seldeslachts, L., Van Weyenbergh, J., De Keyzer, C., Bervoets, L., Sharma, S., Liesenborghs, L., Ma, J., Jansen, S., Van Looveren, D., Vercruysse, T., Wang, X., Jochmans, D., Martens, E., Roose, K., De Vlieger, D., Schepens, B., Van Buyten, T., Jacobs, S., Liu, Y., Martí-Carreras, J., Vanmechelen, B., Wawina-Bokalanga, T., Delang, L., Rocha-Pereira, J., Coelmont, L., Chiu, W., Leyssen, P., Heylen, E., Schols, D., Wang, L., Close, L., Matthijnssens, J., Van Ranst, M., Compernolle, V., Schramm, G., Van Laere, K., Saelens, X., Callewaert, N., Opdenakker, G., Maes, P., Weynand, B., Cawthorne, C., Vande Velde, G., Wang, Z., Neyts, J., Dallmeier, K., 2020. Stat2 signaling restricts viral dissemination but drives severe pneumonia in sars-cov-2 infected hamsters. Nat. Commun. 11, 5838.

Buchrieser, J., Dufloo, J., Hubert, M., Monel, B., Planas, D., Rajah, M.M., Planchais, C., Porrot, F., Guivel-Benhassine, F., Van der Werf, S., Casartelli, N., Mouquet, H., Bruel, T., Schwartz, O., 2020. Syncytia formation by sars-cov-2-infected cells. Embo J. 39, e106267.

Chakraborty, C., Sharma, A.R., Bhattacharya, M., Zayed, H., Lee, S.S., 2021. Understanding gene expression and transcriptome profiling of covid-19: an initiative towards the mapping of protective immunity genes against sars-cov-2 infection. Front. Immunol. 12, 724936.

Chen, N., Zhang, B., Deng, L., Liang, B., Ping, J., 2022. Virus-host interaction networks as new antiviral drug targets for IAV and sars-cov-2. Emerg. Microbes Infect. 11, 1371–1389.

Chen, Y., Liu, Q., Guo, D., 2020. Emerging coronaviruses: genome structure, replication, and pathogenesis. J. Med. Virol. 92, 418–423.

Chevrier, N., Mertins, P., Artyomov, M.N., Shalek, A.K., Iannacone, M., Ciaccio, M.F., Gat-Viks, I., Tonti, E., DeGrace, M.M., Clauser, K.R., Garber, M., Eisenhaure, T.M., Yosef, N., Robinson, J., Sutton, A., Andersen, M.S., Root, D.E., von Andrian, U., Jones, R.B., Park, H., Carr, S.A., Regev, A., Amit, I., Hacohen, N., 2011. Systematic discovery of TLR signaling components delineates viral-sensing circuits. Cell 147, 853–867.

Cucinotta, D., Vanelli, M., 2020. Who declares covid-19 a pandemic. Acta Biomed. 91, 157–160.

Dittmann, M., Hoffmann, H.H., Scull, M.A., Gilmore, R.H., Bell, K.L., Ciancanelli, M., Wilson, S.J., Crotta, S., Yu, Y., Flatley, B., Xiao, J.W., Casanova, J.L., Wack, A., Bieniasz, P.D., Rice, C.M., 2015. A serpin shapes the extracellular environment to prevent influenza a virus maturation. Cell 160, 631–643.

Dobin, A., Davis, C.A., Schlesinger, F., Drenkow, J., Zaleski, C., Jha, S., Batut, P., Chaisson, M., Gingeras, T.R., 2013. Star: ultrafast universal rna-seq aligner. Bioinformatics 29, 15–21.

Fagone, P., Ciurleo, R., Lombardo, S.D., Iacobello, C., Palermo, C.I., Shoenfeld, Y., Bendtzen, K., Bramanti, P., Nicoletti, F., 2020. Transcriptional landscape of sars-cov-2 infection dismantles pathogenic pathways activated by the virus, proposes unique sex-specific differences and predicts tailored therapeutic strategies. Autoimmun. Rev. 19, 102571.

Galluzzi, L., Brenner, C., Morselli, E., Touat, Z., Kroemer, G., 2008. Viral control of mitochondrial apoptosis. PLoS Pathog. 4, e1000018.

Gordon, D.E., Jang, G.M., Bouhaddou, M., Xu, J., Obernier, K., White, K.M., O'Meara, M.J., Rezelj, V.V., Guo, J.Z., Swaney, D.L., Tummino, T.A., Hüttenhain, R., Kaake, R.M., Richards, A.L., Tutuncuoglu, B., Foussard, H., Batra, J., Haas, K., Modak, M., Kim, M., Haas, P., Polacco, B.J., Braberg, H., Fabius, J.M., Eckhardt, M., Soucheray, M., Bennett, M.J., Cakir, M., McGregor, M.J., Li, Q., Meyer, B., Roesch, F., Vallet, T., Mac Kain, A., Miorin, L., Moreno, E., Naing, Z.Z.C., Zhou, Y., Peng, S., Shi, Y., Zhang, Z., Shen, W., Kirby, I.T., Melnyk, J.E., Chorba, J.S., Lou, K., Dai, S.A., Barrio-Hernandez, I., Memon, D., Hernandez-Armenta, C., Lyu, J., Mathy, C.J.P., Perica, T., Pilla, K.B., Ganesan, S.J., Saltzberg, D.J., Rakesh, R., Liu, X., Rosenthal, S.B., Calviello, L., Venkataramanan, S., Liboy-Lugo, J., Lin, Y., Huang, X.-P., Liu, Y., Wankowicz, S.A., Bohn, M., Safari, M., Ugur, F.S., Koh, C., Savar, N.S., Tran, Q.D., Shengjuler, D., Fletcher, S.J., O'Neal, M.C., Cai, Y., Chang, J.C.J., Broadhurst, D.J., Klippsten, S., Sharp, P.P., Wenzell, N.A., Kuzuoglu-Ozturk, D., Wang, H.-Y., Trenker, R., Young, J.M., Cavero, D.A., Hiatt, J., Roth, T.L., Rathore, U., Subramanian, A., Noack, J., Hubert, M., Stroud, R.M., Frankel, A.D., Rosenberg, O.S., Verba, K.A., Agard, D.A., Ott, M., Emerman, M., Jura, N., von Zastrow, M., Verdin, E., Ashworth, A., Schwartz, O., d'Enfert, C., Mukherjee, S., Jacobson, M., Malik, H.S., Fujimori, D.G., Ideker, T., Craik, C.S., Floor, S.N., Fraser, J.S., Gross, J.D., Sali, A., Roth, B.L., Ruggero, D., Taunton, J., Kortemme, T., Beltrao, P., Vignuzzi, M., García-Sastre, A., Shokat, K.M., Shoichet, B.K., Krogan, N.J., 2020a. A sars-cov-2 protein interaction map reveals targets for drug repurposing. Nature 583, 459–468.

Gordon, D.E., Hiatt, J., Bouhaddou, M., Rezelj, V.V., Ulferts, S., Braberg, H., Jureka, A.S., Obernier, K., Guo, J.Z., Batra, J., Kaake, R.M., Weckstein, A.R., Owens, T.W., Gupta, M., Pourmal, S., Titus, E.W., Cakir, M., Soucheray, M., McGregor, M., Cakir, Z., Jang, G., O'Meara, M.J., Tummino, T.A., Zhang, Z., Foussard, H., Rojc, A., Zhou, Y., Kuchenov, D., Hüttenhain, R., Xu, J., Eckhardt, M., Swaney, D.L., Fabius, J.M., Ummadi, M., Tutuncuoglu, B., Rathore, U., Modak, M., Haas, P., Haas, K.M., Naing, Z.Z.C., Pulido, E.H., Shi, Y., Barrio-Hernandez, I., Memon, D., Petsalaki, E., Dunham, A., Marrero, M.C., Burke, D., Koh, C., Vallet, T., Silvas, J.A., Azumaya, C.M., Billesbølle, C., Brilot, A.F., Campbell, M.G., Diallo, A., Dickinson, M.S., Diwanji, D., Herrera, N., Hoppe, N., Kratochvil, H.T., Liu, Y., Merz, G.E., Moritz, M., Nguyen, H.C., Nowotny, C., Puchades, C., Rizo, A.N., Schulze-Gahmen, U., Smith, A.M., Sun, M., Young, I.D., Zhao, J., Asarnow, D., Biel, J., Bowen, A., Braxton, J.R., Chen, J., Chio, C.M., Chio, U.S., Deshpande, I., Doan, L., Faust, B., Flores, S., Jin, M., Kim, K., Lam, V.L., Li, F., Li, J., Li, Y.L., Li, Y., Liu, X., Lo, M., Lopez, K.E., Melo, A.A., Moss 3rd, F.R., Nguyen, P., Paulino, J., Pawar, K.I., Peters, J.K., Pospiech Jr., T.H., Safari, M., Sangwan, S., Schaefer, K., Thomas, P.V., Thwin, A.C., Trenker, R., Tse, E., Tsui, T.K.M., Wang, F., Whitis, N., Yu, Z., Zhang, K., Zhang, Y., Zhou, F., Saltzberg, D., Hodder, A.J., Shun-Shion, A.S., Williams, D.M., White, K.M., Rosales, R., Kehrer, T., Miorin, L., Moreno, E., Patel, A.H., Rihn, S., Khalid, M.M., Vallejo-Gracia, A., Fozouni, P., Simoneau, C.R., Roth, T.L., Wu, D., Karim, M.A., Ghoussaini, M., Dunham, I., Berardi, F., Weigang, S., Chazal, M., Park, J., Logue, J., McGrath, M., Weston, S., Haupt, R., Hastie, C.J., Elliott, M., Brown, F., Burness, K.A., Reid, E., Dorward, M., Johnson, C., Wilkinson, S.G., Geyer, A., Giesel, D.M., Baillie, C., Raggett, S., Leech, H., Toth, R., Goodman, N., Keough, K.C., Lind, A.L., Klesh, R.J., Hemphill, K.R., Carlson-Stevermer, J., Oki, J., Holden, K., Maures, T., Pollard, K.S., Sali, A., Agard, D.A., Cheng, Y., Fraser, J.S., Frost, A., Jura, N., Kortemme, T., Manglik, A., Southworth, D.R., Stroud, R.M., Alessi, D.R., Davies, P., Frieman, M.B., Ideker, T., Abate, C., Jouvenet, N., Kochs, G., Shoichet, B., Ott, M., Palmarini, M., Shokat, K.M., García-Sastre, A., Rassen, J.A., Grosse, R., Rosenberg, O.S., Verba, K.A., Basler, C.F., Vignuzzi, M., Peden, A.A., Beltrao, P., Krogan, N.J., 2020b. Comparative host-coronavirus protein interaction networks reveal pan-viral disease mechanisms. Science 370.

Goshua, G., Pine, A.B., Meizlish, M.L., Chang, C.H., Zhang, H., Bahel, P., Baluha, A., Bar, N., Bona, R.D., Burns, A.J., Dela Cruz, C.S., Dumont, A., Halene, S., Hwa, J., Koff, J., Menninger, H., Neparidze, N., Price, C., Siner, J.M., Tormey, C., Rinder, H.M., Chun, H.J., Lee, A.I., 2020. Endotheliopathy in covid-19-associated coagulopathy: evidence from a single-centre, cross-sectional study. Lancet Haematol. 7, e575–e582.

Hadjadj, J., Yatim, N., Barnabei, L., Corneau, A., Boussier, J., Smith, N., Péré, H., Charbit, B., Bondet, V., Chenevier-Gobeaux, C., Breillat, P., Carlier, N., Gauzit, R., Morbieu, C., Pène, F., Marin, N., Roche, N., Szwebel, T.A., Merkling, S.H., Treluyer, J.M., Veyer, D., Mouthon, L., Blanc, C., Tharaux, P.L., Rozenberg, F., Fischer, A., Duffy, D., Rieux-Laucat, F., Kernéis, S., Terrier, B., 2020. Impaired type i interferon activity and inflammatory responses in severe covid-19 patients. Science 369, 718–724.

Harrison, A.G., Lin, T., Wang, P., 2020. Mechanisms of sars-cov-2 transmission and pathogenesis. Trends Immunol. 41, 1100–1115.

Hu, B., Huang, S., Yin, L., 2021. The cytokine storm and covid-19. J. Med. Virol. 93, 250–256.

Huang, C., Wang, Y., Li, X., Ren, L., Zhao, J., Hu, Y., Zhang, L., Fan, G., Xu, J., Gu, X., Cheng, Z., Yu, T., Xia, J., Wei, Y., Wu, W., Xie, X., Yin, W., Li, H., Liu, M., Xiao, Y., Gao, H., Guo, L., Xie, J., Wang, G., Jiang, R., Gao, Z., Jin, Q., Wang, J., Cao, B., 2020. Clinical features of patients infected with 2019 novel coronavirus in Wuhan, China. Lancet 395, 497–506.

Huang, I.C., Bailey, C.C., Weyer, J.L., Radoshitzky, S.R., Becker, M.M., Chiang, J.J., Brass, A.L., Ahmed, A.A., Chi, X., Dong, L., Longobardi, L.E., Boltz, D., Kuhn, J.H., Elledge, S.J., Bavari, S., Denison, M.R., Choe, H., Farzan, M., 2011. Distinct patterns of ifitm-mediated restriction of filoviruses, sars coronavirus, and influenza a virus. PLoS Pathog. 7, e1001258.

Jia, L., Shi, Y., Wen, Y., Li, W., Feng, J., Chen, C., 2018. The roles of TNFAIP2 in cancers and infectious diseases. J. Cell Mol. Med. 22, 5188–5195.

Keenan, A.B., Torre, D., Lachmann, A., Leong, A.K., Wojciechowicz, M.L., Utti, V., Jagodnik, K.M., Kropiwnicki, E., Wang, Z., Ma'ayan, A., 2019. ChEA3: transcription factor enrichment analysis by orthogonal omics integration. Nucleic Acids Res. 47, W212–w224.

Kolde, R., Laur, S., Adler, P., Vilo, J., 2012. Robust rank aggregation for gene list integration and meta-analysis. Bioinformatics 28, 573–580.

Li, C.X., Gao, J., Zhang, Z., Chen, L., Li, X., Zhou, M., Wheelock Å, M., 2022. Multiomics integration-based molecular characterizations of covid-19. Brief Bioinform 23, bbab485.

Liao, M., Liu, Y., Yuan, J., Wen, Y., Xu, G., Zhao, J., Cheng, L., Li, J., Wang, X., Wang, F., Liu, L., Amit, I., Zhang, S., Zhang, Z., 2020. Single-cell landscape of bronchoalveolar immune cells in patients with covid-19. Nat. Med. 26, 842–844.

Liu, P., Wang, X., Sun, Y., Zhao, H., Cheng, F., Wang, J., Yang, F., Hu, J., Zhang, H., Wang, C.C., Wang, L., 2022. Sars-cov-2 orf8 reshapes the ER through forming mixed disulfides with ER oxidoreductases. Redox Biol. 54, 102388.

Love, M.I., Huber, W., Anders, S., 2014. Moderated estimation of fold change and dispersion for RNA-seq data with deseq2. Genome Biol. 15, 550.

Luck, K., Kim, D.K., Lambourne, L., Spirohn, K., Begg, B.E., Bian, W., Brignall, R., Cafarelli, T., Campos-Laborie, F.J., Charloteaux, B., Choi, D., Coté, A.G., Daley, M., Deimling, S., Desbuleux, A., Dricot, A., Gebbia, M., Hardy, M.F., Kishore, N., Knapp, J.J., Kovács, I.A., Lemmens, I., Mee, M.W., Mellor, J.C., Pollis, C., Pons, C., Richardson, A.D., Schlabach, S., Teeking, B., Yadav, A., Babor, M., Balcha, D., Basha, O., Bowman-Colin, C., Chin, S.F., Choi, S.G., Colabella, C., Coppin, G., D'Amata, C., De Ridder, D., De Rouck, S., Duran-Frigola, M., Ennajdaoui, H.,

Goebels, F., Goehring, L., Gopal, A., Haddad, G., Hatchi, E., Helmy, M., Jacob, Y., Kassa, Y., Landini, S., Li, R., van Lieshout, N., MacWilliams, A., Markey, D., Paulson, J.N., Rangarajan, S., Rasla, J., Rayhan, A., Rolland, T., San-Miguel, A., Shen, Y., Sheykhkarimli, D., Sheynkman, G.M., Simonovsky, E., Taşan, M., Tejeda, A., Tropepe, V., Twizere, J.C., Wang, Y., Weatheritt, R.J., Weile, J., Xia, Y., Yang, X., Yeger-Lotem, E., Zhong, Q., Aloy, P., Bader, G.D., De Las Rivas, J., Gaudet, S., Hao, T., Rak, J., Tavernier, J., Hill, D.E., Vidal, M., Roth, F.P., Calderwood, M.A., 2020. A reference map of the human binary protein interactome. Nature 580, 402–408.

Mahmud, S.M.H., Al-Mustanjid, M., Akter, F., Rahman, M.S., Ahmed, K., Rahman, M.H., Chen, W., Moni, M.A., 2021. Bioinformatics and system biology approach to identify the influences of sars-cov-2 infections to idiopathic pulmonary fibrosis and chronic obstructive pulmonary disease patients. Brief. Bioinform. 22, bbab115.

Mao, G., Zhang, N., 2013. Analysis of average shortest-path length of scale-free network. J. Appl. Math. 2013, 865643.

Mazel-Sanchez, B., Iwaszkiewicz, J., Bonifacio, J.P.P., Silva, F., Niu, C., Strohmeier, S., Eletto, D., Krammer, F., Tan, G., Zoete, V., Hale, B.G., Schmolke, M., 2021. Influenza a viruses balance ER stress with host protein synthesis shutoff. Proc Natl Acad Sci U S A 118, e2024681118.

Miyashita, M., Oshiumi, H., Matsumoto, M., Seya, T., 2011. DDX60, a DEXD/H box helicase, is a novel antiviral factor promoting RIG-I-like receptor-mediated signaling. Mol. Cell Biol. 31, 3802–3819.

Mu, J., Fang, Y., Yang, Q., Shu, T., Wang, A., Huang, M., Jin, L., Deng, F., Qiu, Y., Zhou, X., 2020. Sars-cov-2 n protein antagonizes type I interferon signaling by suppressing phosphorylation and nuclear translocation of STAT1 and STAT2. Cell Discov. 6, 65.

Oshiumi, H., Miyashita, M., Okamoto, M., Morioka, Y., Okabe, M., Matsumoto, M., Seya, T., 2015. DDX60 is involved in RIG-I-dependent and independent antiviral responses, and its function is attenuated by virus-induced EGFR activation. Cell Rep. 11, 1193–1207.

Perrin-Cocon, L., Diaz, O., Jacquemin, C., Barthel, V., Ogire, E., Ramière, C., André, P., Lotteau, V., Vidalain, P.O., 2020. The current landscape of coronavirus-host protein-protein interactions. J. Transl. Med. 18, 319.

Pfefferle, S., Krähling, V., Ditt, V., Grywna, K., Mühlberger, E., Drosten, C., 2009. Reverse genetic characterization of the natural genomic deletion in sars-coronavirus strain Frankfurt-1 open reading frame 7b reveals an attenuating function of the 7b protein in-vitro and in-vivo. Virol. J. 6, 131.

Prelli Bozzo, C., Nchioua, R., Volcic, M., Koepke, L., Krüger, J., Schütz, D., Heller, S., Stürzel, C.M., Kmiec, D., Conzelmann, C., Müller, J., Zech, F., Braun, E., Groß, R., Wettstein, L., Weil, T., Weiß, J., Diofano, F., Rodríguez Alfonso, A.A., Wiese, S., Sauter, D., Münch, J., Goffinet, C., Catanese, A., Schön, M., Boeckers, T.M., Stenger, S., Sato, K., Just, S., Kleger, A., Sparrer, K.M.J., Kirchhoff, F., 2021. Ifitm proteins promote sars-cov-2 infection and are targets for virus inhibition in vitro. Nat. Commun. 12, 4584.

Ramasamy, S., Subbian, S., 2021. Critical determinants of cytokine storm and type I interferon response in covid-19 pathogenesis. Clin. Microbiol. Rev. 34, e00299–20.

Ren, X., Wen, W., Fan, X., Hou, W., Su, B., Cai, P., Li, J., Liu, Y., Tang, F., Zhang, F., Yang, Y., He, J., Ma, W., He, J., Wang, P., Cao, Q., Chen, F., Chen, Y., Cheng, X., Deng, G., Deng, X., Ding, W., Feng, Y., Gan, R., Guo, C., Guo, W., He, S., Jiang, C., Liang, J., Li, Y.-M., Lin, J., Ling, Y., Liu, H., Liu, J., Liu, N., Liu, S.-Q., Luo, M., Ma, Q., Song, Q., Sun, W., Wang, G., Wang, F., Wang, Y., Wen, X., Wu, Q., Xu, G., Xie, X., Xiong, X., Xing, X., Xu, H., Yin, C., Yu, D., Yu, K., Yuan, J., Zhang, B., Zhang, P., Zhang, T., Zhao, J., Zhao, P., Zhou, J., Zhou, W., Zhong, S., Zhong, X., Zhang, S., Zhu, L., Zhu, P., Zou, B., Zou, J., Zuo, Z., Bai, F., Huang, X., Zhou, P., Jiang, Q., Huang, Z., Bei, J.-X., Wei, L., Bian, X.-W., Liu, X., Cheng, T., Li, X., Zhao, P., Wang, F.-S., Wang, H., Su, B., Zhang, Z., Qu, K., Wang, X., Chen, J., Jin, R., Zhang, Z., 2021. Covid-19 immune features revealed by a large-scale single-cell transcriptome atlas. Cell 1895–1913.e19.

Sano, R., Reed, J.C., 2013. Er stress-induced cell death mechanisms. Biochim. Biophys. Acta 1833, 3460–3470.

Shi, G., Kenney, A.D., Kudryashova, E., Zani, A., Zhang, L., Lai, K.K., Hall-Stoodley, L., Robinson, R.T., Kudryashov, D.S., Compton, A.A., Yount, J.S., 2021. Opposing activities of IFITM proteins in sars-cov-2 infection. Embo J. 40, e106501.

Stuart, T., Butler, A., Hoffman, P., Hafemeister, C., Papalexi, E., Mauck 3rd, W.M., Hao, Y., Stoeckius, M., Smibert, P., Satija, R., 2019. Comprehensive integration of single-cell data. Cell 177, 1888–1902.e1821.

Su, G., Morris, J.H., Demchak, B., Bader, G.D., 2014. Biological network exploration with Cytoscape 3. Curr. Protoc. Bioinform. 47, 8.13.11-24.

Sun, J., Ye, F., Wu, A., Yang, R., Pan, M., Sheng, J., Zhu, W., Mao, L., Wang, M., Xia, Z., Huang, B., Tan, W., Jiang, T., 2020. Comparative transcriptome analysis reveals the intensive early stage responses of host cells to sars-cov-2 infection. Front. Microbiol. 11, 593857.

Suryawanshi, R.K., Koganti, R., Agelidis, A., Patil, C.D., Shukla, D., 2021. Dysregulation of cell signaling by sars-cov-2. Trends Microbiol. 29, 224–237.

Tan, S.L., Ganji, G., Paeper, B., Proll, S., Katze, M.G., 2007. Systems biology and the host response to viral infection. Nat. Biotechnol. 25, 1383–1389.

Terracciano, R., Preianò, M., Fregola, A., Pelaia, C., Montalcini, T., Savino, R., 2021. Mapping the sars-cov-2-host protein-protein interactome by affinity purification mass spectrometry and proximity-dependent biotin labeling: a rational and straightforward route to discover host-directed anti-sars-cov-2 therapeutics. Int. J. Mol. Sci. 22, 532.

Wang, X., Xu, G., Liu, X., Liu, Y., Zhang, S., Zhang, Z., 2021. Multiomics: unraveling the panoramic landscapes of sars-cov-2 infection. Cell. Mol. Immunol. 18, 2313–2324.

Wettstein, L., Weil, T., Conzelmann, C., Müller, J.A., Groß, R., Hirschenberger, M., Seidel, A., Klute, S., Zech, F., Prelli Bozzo, C., Preising, N., Fois, G., Lochbaum, R., Knaff, P.M., Mailänder, V., Ständker, L., Thal, D.R., Schumann, C., Stenger, S., Kleger, A., Lochnit, G., Mayer, B., Ruiz-Blanco, Y.B., Hoffmann, M., Sparrer, K.M.J., Pöhlmann, S., Sanchez-Garcia, E., Kirchhoff, F., Frick, M., Münch, J., 2021. Alpha-1 antitrypsin inhibits TMPRSS2 protease activity and sars-cov-2 infection. Nat. Commun. 12, 1726.

Wrensch, F., Winkler, M., Pöhlmann, S., 2014. IFITM proteins inhibit entry driven by the MERS-coronavirus spike protein: evidence for cholesterol-independent mechanisms. Viruses 6, 3683–3698.

Wu, A., Peng, Y., Huang, B., Ding, X., Wang, X., Niu, P., Meng, J., Zhu, Z., Zhang, Z., Wang, J., Sheng, J., Quan, L., Xia, Z., Tan, W., Cheng, G., Jiang, T., 2020. Genome composition and divergence of the novel coronavirus (2019-ncov) originating in China. Cell Host Microbe 27, 325–328.

Xia, H., Cao, Z., Xie, X., Zhang, X., Chen, J.Y., Wang, H., Menachery, V.D., Rajsbaum, R., Shi, P.Y., 2020. Evasion of type i interferon by sars-cov-2. Cell Rep. 33, 108234.

Yang, H., Rao, Z., 2021. Structural biology of sars-cov-2 and implications for therapeutic development. Nat. Rev. Microbiol. 19, 685–700.

Yu, G., Wang, L.G., Han, Y., He, Q.Y., 2012. Clusterprofiler: an R package for comparing biological themes among gene clusters. OMICS 16, 284–287.

Zhang, J., Cruz-Cosme, R., Zhuang, M.W., Liu, D., Liu, Y., Teng, S., Wang, P.H., Tang, Q., 2020a. A systemic and molecular study of subcellular localization of sars-cov-2 proteins. Signal Transduct. Target. Ther. 5, 269.

Zhang, P., Su, C., Jiang, Z., Zheng, C., 2017. Herpes simplex virus 1 UL41 protein suppresses the IRE1/XBP1 signal pathway of the unfolded protein response via its RNase Activity. J. Virol. 91, e02056–16.

Zhang, X., Tan, Y., Ling, Y., Lu, G., Liu, F., Yi, Z., Jia, X., Wu, M., Shi, B., Xu, S., Chen, J., Wang, W., Chen, B., Jiang, L., Yu, S., Lu, J., Wang, J., Xu, M., Yuan, Z., Zhang, Q., Zhang, X., Zhao, G., Wang, S., Chen, S., Lu, H., 2020b. Viral and host factors related to the clinical outcome of covid-19. Nature 583, 437–440.

Zhang, Y., Chen, Y., Li, Y., Huang, F., Luo, B., Yuan, Y., Xia, B., Ma, X., Yang, T., Yu, F., 2021a. The ORF8 protein of sars-cov-2 mediates immune evasion through down-regulating MHC-ι. Proc. Natl. Acad. Sci. U. S. A. 118, e2024202118.

Zhang, Z., Ye, S., Wu, A., Jiang, T., Peng, Y., 2021b. Prediction of the receptorome for the human-infecting virome. Virol. Sin. 36, 133–140.

Zuo, Y., Warnock, M., Harbaugh, A., Yalavarthi, S., Gockman, K., Zuo, M., Madison, J.A., Knight, J.S., Kanthi, Y., Lawrence, D.A., 2021. Plasma tissue plasminogen activator and plasminogen activator inhibitor-1 in hospitalized covid-19 patients. Sci. Rep. 11, 1580.